

晶体铅动力学及其表面性质的势能函数模拟

李思殿¹, 金志浩², H. 考可斯³, J. N. 谟若³

(1. 西安交通大学材料科学与工程学院, 陕西 西安 710049; 2. 山西忻州师范学院化学系, 山西 忻州 034000;
3. 英国萨塞克斯大学化学和分子科学院, 布莱顿 BN1 9QJ, UK)

摘要:采用优化的多体展开势能函数研究面心立方(FCC)晶体铅的动力学和表面性质。在(q00), (qq0)及(qqq)高对称方向, 计算声子散射频率与实验曲线良好吻合。Pb(110)表面弛豫严重, 其最外层原子向内压缩率达18%。表面7层存在压缩-膨胀交替现象。蒙特卡罗模拟表明, FCC铅在425K开始熔化, 模拟结果比纳米铅低约25K。

关键词:多体展开势能函数; 铅; 声子散射; 表面性质; 熔化温度

中图分类号: O 561.1

文献标识码: A

文章编号: 1001-4160(2002)06-759-762

A potential energy function study of the dynamical and surface properties of lead

LI Si-dian¹, JIN Zhi-hao², Hazel Cox³ and J. N. Murrell³

(1. School of Materials Science and Engineering, Xian Jiaotong University, Xian 710049, Shanxi, China; 2. Department of Chemistry, Xinzhou Teachers' University, Xinzhou, 034000, Shanxi, China; 3. School of Chemistry and Molecular Sciences, University of Sussex, Brighton BN1 9QJ, UK)

Abstract: A many-body potential energy function has been employed to investigate the dynamical properties, surface energies and reconstructions, and melting behavior of face-centered cubic (FCC) lead. Experimental phonon dispersion curves along (q00), (qq0) and (qqq) high symmetry directions are well reproduced. Surface energy calculations indicate that Pb(110) undergoes a severe surface relaxation. A large inward relaxation up to -18% relative to FCC lattice is predicted for the top-most layer of Pb(110) surface and an expansion-contraction alternation for the top 7 interlayer spaces is observed. Monte Carlo simulation indicates that FCC lead melt above 425K with this potential, an estimation about 25K lower than the observed melting point of Pb nano-particles.

Keywords: many-body potential energy function; Pb; phonon dispersion; surface property; melting temperature

1 Introduction

As a heavy metal, the dynamic properties of lead are featured in two aspects. Firstly, it is the first material for which the profound Kohn anomalies in the (qqq)L branch near the point of (0.5, 0.5, 0.5) were observed, and secondly, the strong long range phonon-electron interaction causes strong curvature near the Brillouin zone boundaries along both (q00) and (qq0) directions^[1,2]. Fitting the phonon dispersion curves of the face-centered cubic (FCC) lead has remained as a big challenge to various kinds of theories so far. The 26 Born-Von Karman (BVK) force constants obtained with a phenomenological

fit by Cowley^[2] reproduced the general shape of the observed phonon dispersion curves along high symmetry directions, but failed to reproduce the Kohn anomalies and the long range electron-phonon interaction. An energy dependent pseudo-potential was employed to fit the phonon dispersion curves of lead later by So and co-workers^[3], but their fitting was obviously worse than Cowley's parameterized BVK model.

FCC lead undergoes pressure-induced phase transitions (FCC - > HCP - > BCC) and the three kinds of solids lie very close in cohesive energies (within 0.026 eV per atom), while the diamond structure, which is the most

收稿日期: 2002-06-28; 修回日期: 2002-10-12

作者简介: 李思殿 (1959—), 男, 教授, 硕士生导师。

stable form for other group IV elements, is much less stable for Pb due to the strong relativistic effect^{4,5}. Surface energies of Pb (110) and (111) were predicted to be almost the same and a very large inward relaxation for the top layer in (110) direction were also confirmed by both experiment and theory⁶. An very recent in situ high-resolution electron microscopy observation by Mitome⁷ has shown that nano-meter lead particles with diameters of 6 nm melt into liquid in the core region at just above 443K (170°C), well below the melting point of the bulk (600.7K). Surface-initiated pre-melting at 450K was also observed on Pb(110) by Frenken's group⁸.

In this work, we utilize the 2 + 3 body effective potential energy function proposed by Murrell and CO - workers⁹⁻¹¹ to study the dynamic properties of FCC lead, to calculate the surface energies and surface relaxations, and to simulate the surface melting process. We aim to provide a simple analytical function that can be used to predict various kinds of properties of solid lead.

2 Optimization of the Potential

The 2 + 3 body effective potential energy function has been documented in a large number of publications^[9-10]. Various applications of the potential can be found in a recent comprehensive review^[11] and the references cited therein.

The full potential of the lattice is written as the sum of the 2-body $V_{ij}^{(2)}$ and 3-body $V_{ijk}^{(3)}$ terms

$$V = \sum_i \sum_j V_{ij}^{(2)} + \sum_i \sum_j \sum_k V_{ijk}^{(3)} \quad (1)$$

Where

$$V_{ij}^{(2)} = -D_e(1 + a_2 \rho_{ij}) \exp(-a_2 \rho_{ij}) \quad (2)$$

$$\rho_{ij} = (r_{ij} - r_e)/r_e \quad (3)$$

and

$$\begin{aligned} V_{ijk}^{(3)} = & D_e \{ C_0 + C_1 Q_1 \\ & + C_2 Q_1^2 + C_3 (Q_2^2 + Q_3^2) + C_4 Q_1^3 \\ & + C_5 Q_1 (Q_2^2 + Q_3^2) + C_6 (Q_3^3 - 3 Q_3 Q_2^2) \\ & + C_7 Q_1^4 + C_8 Q_1^2 (Q_2^2 + Q_3^2) + C_9 (Q_2^2 + Q_3^2)^2 \\ & + C_{10} Q_1 (Q_3^3 - 3 Q_3 Q_2^2) \} \\ \text{Damp}(a_3, Q_1) \end{aligned} \quad (4)$$

r_e and D_e are distance and energy scaling factors respec-

tively which ensure that the lattice constants and cohesive energies of the bulk are reproduced exactly, a_2 and a_3 are adjustable exponents for two and three body terms respectively, while (Q_1, Q_2, Q_3) are the so-called symmetry coordinates. The damping function Damp chosen for lead in this work is a Gauss-type function^[11].

Table 1 The optimized parameters of the quartic 2 + 3 body potential used in this work

a_2	7.6	C_3	-4.833387
a_3	4.2	C_4	-7.298921
D_e/eV	0.58795	C_5	10.550173
$R_e/\text{\AA}$	3.30719	C_6	0.608533
		C_7	6.687216
C_0	0.546760	C_8	-11.653804
C_1	-1.214105	C_9	3.106570
C_2	3.598935	C_{10}	-1.866951

The above process has been programmed and detailed description of the parameter optimization procedure can be found in Ref [11]. The optimized parameters of the quartic potential used in this work are listed in Table 1.

3 Results and discussion

This potential reproduces the phonon dispersion curves of FCC Pb (q00), (qq0) and (qqq) quite well (see Fig.1). As can be seen from the figure, the Kohn anomalies at the top-most branch near point L (0.5, 0.5, 0.5) and the long range electron-phonon interaction at the zone boundary (1, 0, 0) have also been fairly well represented. The calculated curves approach the shadow minima at (1, 0, 0) for both the L and T_2 branches at the same time although the fit is not perfect. Our potential has much fewer adjustable parameters compared to the BCM model^[2] which simply treated all the 26 force constants as adjustable parameters in a phenomenological fit. Instead, we calculated force constants with the parameterized model potential.

This potential produces almost the same cohesive energies for FCC (2.0300 eV), HCP (2.0203 eV) and BCC (2.0300 eV) lead, in agreement with previous results obtained in references mentioned above. While diamond structure, the most stable form of C, Si, G_e at room temperature, is very unstable for Pb (1.53 eV). The calcu-

lated elastic constants C_{11} , C_{12} and C_{44} , and vacancy energy E_{coh} are 0.5102, 0.4457, 0.1972 (eV \AA^{-3}) and 0.49 (eV) respectively, agreeing well with the corresponding experimental values of 0.5386, 0.4460, 0.1804 (eV \AA^{-3}) and 0.50 (eV).

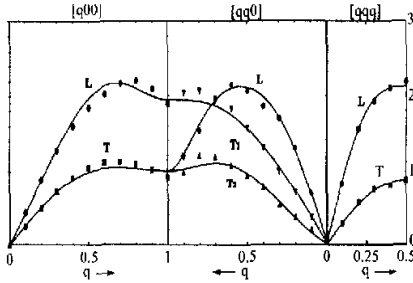


Fig.1 The calculated phonon frequencies of FCC Pb (real lines) compared to experimental values (real circles, triangles, and squares) along $(q00)$, $(qq0)$ and (qqq) high symmetry directions

Table 2 The calculated un-relaxed and relaxed surface energies γ (meV \AA^{-2}) of FCC lead compared with corresponding experimental values

Surface	Un-relaxed	Relaxed	Ref[6]	Ref[13]	Exp[14]
(100)	41.22	39.01	38.0		
(110)	41.53	37.99	41.8	35.0	37.3
(111)	35.22	35.01	37.5	31.0	(extrapolated)

Surface energies γ of Pb (100), (110) and (111) are calculated by directly applying the optimized potential. The calculated results are compared in Table 2 with other theoretical results and corresponding experimental values. The comparison is satisfactory. Our calculated surface energy for the relaxed FCC (110) is $37.99 \text{ meV \AA}^{-2}$, very close to the experimental value of $37.3 \text{ meV \AA}^{-2}$ [12]. We obtained an anisotropy in surface energy (defined as $\gamma(110)/\gamma(111)$) of 1.09 for Pb, also in good agreement with the value of 1.10 for FCC Pb in Ref [9]. This is reasonable because Pb (111) surface is close - packed while (110) surface is less flat. The small anisotropy for Pb is quite close to the value of 1.10 for FCC Al[13].

Table 3 The surface relaxation of FCC lead in percentage compared with experiments

Surfaces	(110)		(100)	(111)
	this work	exp [14]		
d_{12}	-18.25	-16.3	-6.77	-2.17
d_{23}	+10.88	+3.4	+3.23	+0.26
d_{34}	-7.59	-4.0	-0.97	+0.01
d_{45}	+4.93		+0.46	+0.05
d_{56}	-2.90		-0.03	
d_{67}	+1.65			
d_{78}	-0.43			

Large relaxations are obtained for lead surfaces (see Table 3). Severe inward contraction of the top-most layer of (110) surface reaches about -18.3% relative to perfect FCC (110) inter-layer spacing, very close to the experimental value of -16.3%[14]. The second inter-layer spacing expands about +10%. Experimentally, it expands about +3.4%. For the third inter-layer spacing, the calculated value of -7.6% contraction also qualitatively agree with corresponding experimental result of -4.0%. The general trend of calculated results agrees with available experiments and the contraction and expansion alternation of inter-layer spacing has been well reproduced.

Reconstruction of Pb (110) surface is an interesting topic in interpreting the surface properties of the bulk. Reconstructions of the un-relaxed and relaxed surface are compared in Table 4. Both (1×2) and (1×3) reconstructions are unfavored in energies when compared with the relaxed (110) surface. The relaxed Pb (110) has a surface energy of $37.99 \text{ meV \AA}^{-2}$ (see Table 2), lower than both the surface energies of 40.60 for (1×2) reconstruction and 41.37 for (1×3) reconstruction.

Table 4 Surface energies of the un-relaxed and relaxed reconstructed Pb (110) surfaces

Reconstruction	Un-relaxed	Relaxed
1×2	42.16	40.60
1×3	42.49	41.37

This result is in accordance with Prince's[15] experimental observation that no reconstruction was observed with

potassium adsorption on Pb (110) surface when examined with LEED and AES. As mentioned in by Barnes¹⁶, instead of surface reconstruction, sp-band FCC metals like Al and Pb exhibit (1 × 1) bulk truncation when clean with quite large interlayer relaxations¹³.

A Monte Carlo simulation was performed to study the melting behavior of bulk lead based upon a 8-layer slab containing $5 \times 5 \times 8 = 200$ atoms with periodic boundary conditions in x , y and z three dimensions. To ensure that the system reaches its equilibrium state at specific temperatures, three quantities including the averaged order parameter S relative to the ideal FCC lattice, the energy evolution of the simulated system, and the radial distribution function, are used to monitor the simulation process. The variation of the bulk order parameter S with temperature T is shown in Fig.2. A sharp change of the order parameter with temperature occurs between $T = 375\text{K}$ ($S = 0.8$) and 425K ($S = 0.06$) has clearly indicated a phase transition from the ordered FCC lattice to a disordered liquid phase. At temperatures above 425K , S values are steadily smaller than 0.07 and the radial distribution are typical of liquids, indicating that FCC lead is melt above 425K with this potential. This estimation is about 25K lower than the pre-melting temperature 443K observed in the core region of 6 nm Pb particles by Mitome⁷ and surface-initiated pre-melting at about 450K observed in Ref [8]. Melting temperatures vary with the size of the particles studied. We predict that, with nanometer Pb particles smaller than 6 nm in diameters, the melting temperature of Pb may be even lower than 443K .

Further investigations to apply the 2 + 3 body effective potential to micro-sized and medium-sized Pb_n clusters ($n = 2\text{--}200$) and similar systems¹⁷ and gas-solid interface interactions are under progress.

References

- 1 Stedman R, Almqvist L, Nilsson C. Phys Rev, 1967, 162: 549.
- 2 Cowley F R. Solid State Communication, 1974, 14: 587.
- 3 So C B, Wang S. J Phys. F: Metal Phys, 1977, 7: 35.
- 4 Christensen N E, Satphay S, Pawlowska Z. Phys Rev, 1986, B34: 5977.
- 5 Liu A Y, Garcia A, Cohen M L, Godwal B K, Jeanloz R. Phys Rev, 1991, B43: 1795.
- 6 Mansfield M, Needs R J. Phys Rev, 1991, B43: 8829.
- 7 Mitome M. Surf Sci, 1999, 442 (1): L953.
- 8 Frenken J W M, Maree P M J, Ven der veeen J F. Phys Rev, 1986, B34: 7506.
- 9 Murrell J N, Mottram R E. Mol Phys, 1990, 69: 571.
- 10 Li Sidian, Johnston R, Murrell J N. J Chem Soc, Faraday Trans, 1992, 88: 1229.
- 11 Cox H, Johnston R L, Murrell J N. J Solid State Chem, 1999, 145: 517.
- 12 Tyson W R, Miller W A. Surf Sci, 1977, 62: 267.
- 13 Lim H S, Ong C K, Ercolessi F. Surf Sci, 1992, 37: 1109.
- 14 Li Y S, Quinn J, Jona F, Marcus P M. Phys Rev, 1989, B40: 8239.
- 15 Prince K C. Surf Sci, 1988, 193: T24.
- 16 Barnes C J. The chemical physics of solid surfaces. Edited by King D A and Woodduff D P. Elsevier: Amsterdam, 1994: 501.
- 17 Fournier R. J Chem Phys, 2001, 115: 2165.

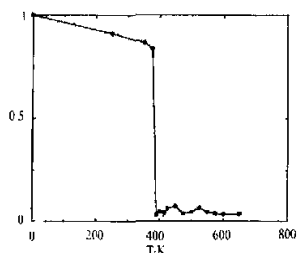


Fig.2 Variation of the calculated order parameter S vis temperature T

晶体铅动力学及其表面性质的势能函数模拟

作者: [李思殿](#), [金志浩](#), [H·考可斯](#), [J·N·谟若](#)

作者单位: [李思殿\(西安交通大学材料科学与工程学院, 陕西, 西安, 710049\)](#), [金志浩\(山西忻州师范学院化学系, 山西, 忻州, 034000\)](#), [H·考可斯, J·N·谟若\(英国萨塞克斯大学化学和分子科学院, 布莱顿, BN19QJ, UK\)](#)

刊名: [计算机与应用化学](#) **ISTIC PKU**

英文刊名: [COMPUTERS AND APPLIED CHEMISTRY](#)

年, 卷(期): 2002, 19(6)

参考文献(17条)

1. [Stedman R;Almqvist L;Nilsson G](#) [查看详情](#) [外文期刊] 1967
2. [Cowley E R](#) [查看详情](#) [外文期刊] 1974
3. [So C B;Wang S](#) [查看详情](#) [外文期刊] 1977
4. [Christensen N E;Satpthy S;Pawlowska Z](#) [查看详情](#) 1986
5. [Liu A Y;Garcia A;Cohen M L;Godwal B K, Jeanloz R](#) [查看详情](#) 1991
6. [Mansfield M;Needs R J](#) [查看详情](#) 1991
7. [Mitome M](#) [查看详情](#) 1999(01)
8. [Frenken J W M;Maree P M J;Ven der veen J F](#) [查看详情](#) 1986
9. [Murrell J N;Mottram R E](#) [查看详情](#) 1990
10. [Li Sidian;Johnston R;Murrell J N](#) [查看详情](#) [外文期刊] 1992
11. [Cox H;Johnston R L;Murrell J N](#) [查看详情](#) 1999
12. [Tyson W R;Miller W A](#) [查看详情](#) [外文期刊] 1977
13. [LimHS;OngCK;Ercolessi F](#) [查看详情](#) 1992
14. [LI YS;QuinnJ;JonaF;MarcusPM](#) [查看详情](#) 1989
15. [Prince K C](#) [查看详情](#) 1988
16. [Barnes C J](#); Edited by [King D A](#); [Woodduff D P](#) [The chemical physics of solid surfaces](#) 1994
17. [Fournier R](#) [Theoretical study of the structure of silver clusters](#) [外文期刊] 2001(5)

本文链接: http://d.g.wanfangdata.com.cn/Periodical_jsjyyhx200206024.aspx